

Forecasting range shifts of a dioecious plant species under climate change

Jacob K. Moutouama ^{*1}, Aldo Compagnoni², and Tom E.X. Miller¹

¹Program in Ecology and Evolutionary
Biology, Department of BioSciences, Rice University, Houston, TX USA

²Institute
of Biology, Martin Luther University Halle-Wittenberg, Halle, Germany; and
German Centre for Integrative Biodiversity Research (iDiv), Leipzig, Germany

Running header: Forecasting range shifts

Keywords: climate change, demography, forecasting, matrix projection model, mechanistic models, sex ratio, range limits

Acknowledgements: This research was supported by XX.

Authorship statement: XXXXX.

Data accessibility statement: All data (Miller and Compagnoni, 2022a) used in this paper are publicly available. Should the paper be accepted, all computer scripts supporting the results will be archived in a Zenodo package, with the DOI included at the end of the article. During peer review, our data and code are available at <https://github.com/jmoutouama/POAR-Forecasting>.

Conflict of interest statement: None.

^{*}Corresponding author: jmoutouama@gmail.com

¹ Abstract

² Rising temperatures and extreme drought events associated with global climate change have
³ triggered an urgent need for predicting species response to climate change. Currently, the
⁴ vast majority of theory and models in population biology, including those used to forecast
⁵ biodiversity responses to climate change, ignore the complication of sex structure. To address
⁶ this issue, we developed a climate-driven population matrix model using demographic data of
⁷ dioecious species (Texas bluegrass), past and future climate (different gas emission scenarios)
⁸ to forecast and backcast the effect of climate change on range shifts. Our results show a sex
⁹ specific demographic response to climate change. Female individuals have a demographic
¹⁰ advantage (higher vital rate) over males. Female demographic advantage led to a slight
¹¹ decline in population viability under future climate assuming moderate gas emission and
¹² a drastic reduction in population viability under future climate assuming high gas emission.
¹³ Despite a change in species range, climate change can alter population viability in dioecious
¹⁴ species. Overall, our work provides a framework for predicting the impact of climate on
¹⁵ dioecious species using population demography.

¹⁶ Introduction

¹⁷ Rising temperatures and extreme drought events associated with global climate change are
¹⁸ leading to increased concern about how species will become redistributed across the globe
¹⁹ under future climate conditions (Bertrand et al., 2011; Gamelon et al., 2017; Smith et al., 2024).
²⁰ Dioecious species (most animals and many plants) might be particularly vulnerable to the
²¹ influence of climate change because they often display skewed sex ratios that are generated or
²² reinforced by sexual niche differentiation (distinct responses of females and males to shared cli-
²³ mate drivers) (Tognetti, 2012). Accounting for such a niche differentiation within a population
²⁴ is a long-standing challenge in accurately predicting which sex will successfully track envi-
²⁵ ronmental change and how this will impact population viability and range shifts (Gissi et al.,
²⁶ 2023a; Jones et al., 1999). The vast majority of theory and models in population biology, includ-
²⁷ ing those used to forecast biodiversity responses to climate change, ignore the complication of
²⁸ sex structure (Ellis et al., 2017; Pottier et al., 2021). As a result, accurate forecasts of colonization-
²⁹ extinction dynamics for dioecious species under future climate scenarios are limited.

³⁰ Climate change can influence dioecious populations via shifts in sex ratio.¹ Females and
³¹ males may respond differently to climate change, especially in species where there is sexual
³² niche differentiation (Gissi et al., 2023a,b; Hultine et al., 2016). This sex-specific response to
³³ climate change may help one sex to succeed in extreme climatic conditions rather than the
³⁴ other sex (Bürli et al., 2022; Zhao et al., 2012) leading to a skewness in the operational sex ratio
³⁵ (relative number of males and females as available mates) (Eberhart-Phillips et al., 2017). For
³⁶ example, experiments in two populations of Atlantic marine copepods (*Acartia tonsa*) revealed
³⁷ that male survival was more sensitive to increasing temperatures than female survival (Sasaki
³⁸ et al., 2019). In other species, such as *Pteropus poliocephalus* or *Populus cathayana*, females
³⁹ showed lower survival than males in response to high temperature (Welbergen et al., 2008;
⁴⁰ Zhao et al., 2012). Sex-specific responses to climate drivers have the potential to influence
⁴¹ population viability under global change because skew in the operational sex ratio can limit
⁴² reproduction through mate scarcity (Petry et al., 2016).

⁴³ Species's range limits, when not driven by dispersal limitation, should generally reflect
⁴⁴ the limits of the ecological niche (Lee-Yaw et al., 2016). For most species, niches and geographic
⁴⁵ ranges are often limited by climatic factors including temperature and precipitation (Sexton
⁴⁶ et al., 2009). Therefore, any substantial changes in the magnitude of these climatic factors in a
⁴⁷ given location across the range could impact population viability, with implications for range
⁴⁸ shifts based on which regions become more or less suitable (Davis and Shaw, 2001; Pease

¹This paragraph is really good but notice that the topic sentence (and much that follows) is largely redundant with the first paragraph. I would suggest creating clearer distinction between paragraphs.

49 et al., 1989). Forecasting range shifts for dioecious species is complicated by the potential for
50 each sex to respond differently to climate variation (Morrison et al., 2016; Pottier et al., 2021).
51 Populations in which males are rare under current climatic conditions could experience low
52 reproductive success due to sperm or pollen limitation that may lead to population decline in
53 response to climate change that disproportionately favors females (Eberhart-Phillips et al., 2017).
54 In contrast, climate change could expand male habitat suitability (e.g. upslope movement),
55 which might increase seed set for pollen-limited females and favor range expansion (Petry
56 et al., 2016). Although the response of species to climate warming is an urgent and active area
57 of research, few studies have disentangled the interaction between sex and climate drivers
58 to understand their combined effects on population dynamics and range shifts.

59 Our ability to track the impact of climate change on the population dynamics of
60 dioecious plants and the implication of such impact on range shift depends on our ability
61 to build mechanistic models that take into account the spatial and temporal context in which
62 sex specific response to climate change affects population viability (Czachura and Miller, 2020;
63 Davis and Shaw, 2001; Evans et al., 2016). For example, structured models that are built from
64 long-term demographic data collected from common garden experiments have emerged as
65 powerful technic to study the impact of climate change on species range shift (Merow et al.,
66 2017; Schwinning et al., 2022). These structured models are increasingly utilized for two
67 reasons. First, they enable the manipulation of treatments that can isolate spatial and temporal
68 correlations between environmental factors, thus overcoming a main disadvantage with many
69 types of correlative studies (Leicht-Young et al., 2007). Second, they link individual-level
70 demographic trait to population demography allowing the investigation of the demographic
71 mechanisms behind vital rates (e.g. survival, fertility, growth and seed germination) response
72 environmental variation (Dahlgren et al., 2016; Louthan et al., 2022).

73 In this study, we used a mechanistic approach by combining geographically-distributed
74 field experiments, hierarchical statistical modeling, and two-sex population projection
75 modeling to understand the demographic response of dioecious species to climate change and
76 its implications for future range dynamics. Our study system is a dioecious plant species (*Poa*
77 *arachnifera*) distributed along environmental gradients in the south-central US corresponding
78 to variation in temperature across latitude and precipitation across longitude. A previous
79 study on the same system showed that, despite a differentiation of climatic niche between
80 sexes, the female niche mattered the most in driving the environmental limits of population
81 viability (Miller and Compagnoni, 2022b). However that study did not use climate variables
82 preventing us from backcasting and forecasting the impact of climate change on dioecious
83 species. Here, we asked four questions:

- 84 1. What are the sex-specific vital rate responses to variation in temperature and precipitation
85 across the species' range?
- 86 2. How sex-specific vital rates combine to determine the influence of climate variation on
87 population viability (λ)?
- 88 3. What are the historical and projected changes in climate across the species range?
- 89 4. What are the back-casted and fore-casted dynamics of this species' geographic niche
90 ($\lambda \geq 1$) and how does accountind for sex structure modify these predictions?

91 Materials and methods

92 Study species

93 Texas bluegrass (*Poa arachnifera*) is a dioecious perennial, summer-dormant cool-season (C3)
94 grass that occurs in the south-central U.S.(Texas, Oklahoma, and southern Kansas) (Hitchcock,
95 1971). Average temperatures along the distribution of the species tend to decrease northward
96 as a result of the influence of latitude: lower latitudes receive more heat from the sun over
97 the course of a year. Similarly the average precipitation decrease eastward as a result of
98 the influence of longitude: lower longitudes receive less precipitation over the year. Texas
99 bluegrass grows between October and May (growing season), with onset of dormancy often
100 from June to September (dormant season) (Kindiger, 2004). Flowering occurs in May and
101 the species is wind pollinated (Hitchcock, 1971). **The male heads are smooth, while those
102 of the female appear fuzzy.**

103 Common garden experiment

104 We set up a common garden experiment throughout and beyond the range of Texas bluegrass
105 to enable study of sex-specific demographic responses to climate and the implications for range
106 shifts. The novelty of this study lies in the fact that we use a precise climate variable to build
107 a mechanistic model to forecast the response of species to climate change. Details of the exper-
108 imental design are provided in Miller and Compagnoni (2022b); we provide a brief overview
109 here. The common experiment was installed at 14 sites across a climatic gradient (FigX). At
110 each site, we established 14 blocks. For each block we planted three female and three male indi-
111 viduals that were clonally propagated from eight natural source populations of Texas bluegrass.
112 The experiment was established in November 2013 and was census annually through 2016, pro-
113 viding both spatial and inter-annual variation in climate. Each May (2014-2016), we collected
114 individual demographic data including survival (alive or dead), growth (number of tillers),

¹¹⁵ flowering status (reproductive or vegetative), and fertility (number of panicles, conditional on
¹¹⁶ flowering). For the analyses that follow, we focus on the 2014-15 and 2015-16 transitions years.

¹¹⁷ Climatic data collection

¹¹⁸ We downloaded monthly temperature and precipitation from Chelsa to describe observed
¹¹⁹ climate conditions during our study period (Karger et al., 2017). These climate data were used
¹²⁰ as covariates in vital rate regressions, which allowed us to forecast and back-cast demographic
¹²¹ responses to climate change based on observations across the common garden experiment.
¹²² We aligned the climatic years to match demographic transition years (**May 1 – April 30**)²
¹²³ rather than calendar years. Based on the natural history of this summer-dormant cool-season
¹²⁴ species, we divided each transition year into growing and dormant seasons. We define June
¹²⁵ through September as the dormant season and the rest of the year as the growing season.
¹²⁶ Across years and sites, the experiment included substantial variation in growing and dormant
¹²⁷ season temperature and precipitation (**Figure**³).

¹²⁸ To back-cast and forecast changes in climate, we downloaded projection data for three
¹²⁹ 30-year periods: past (1901-1930), current (1990-2019) and future (2070-2100). Data for these
¹³⁰ climatic periods were downloaded from four general circulation models (GCMs) selected
¹³¹ from the Coupled Model Intercomparison Project Phase 5 (CMIP5). The GCMs are MIROC5,
¹³² ACCESS1-3, CESM1-BGC, CMCC-CM and were downloaded from chelsa (Sanderson
¹³³ et al., 2015). We evaluated future climate projections from two scenarios of representative
¹³⁴ concentration pathways (RCPs): RCP4.5, an intermediate-to-pessimistic scenario assuming
¹³⁵ a radiative forcing to amount to 4.5 W m^{-2} by 2100, and RCP8.5, a pessimistic emission
¹³⁶ scenario which project a radiative forcing to amount to 8.5 W m^{-2} by 2100 (Schwalm et al.,
¹³⁷ 2020; Thomson et al., 2011).

¹³⁸ Sex ratio experiment

¹³⁹ We conducted a sex-ratio experiment on a site close (1 km) to a natural population of the
¹⁴⁰ focal species at the center of the range to estimate the effect of sex-ratio variation on female
¹⁴¹ reproductive success. Details of the experiment are provided in Compagnoni et al. (2017) and
¹⁴² Miller and Compagnoni (2022b). In short, we established 124 experimental populations on
¹⁴³ plots measuring $0.4 \times 0.4\text{m}$ and separated by at least 15m from each other at that site. We chose
¹⁴⁴ 15m because our pilot data show that more than 90% of wind pollination occurred within 13m.

²I am not sure if these are actually the right dates.

³I think we should have a figure, maybe just for the appendix, that visualizes this.

¹⁴⁵ We varied population density (1-48 plants/plot) and sex ratio (0%-100% female) across the ex-
¹⁴⁶ perimental populations, and we replicated 34 combinations of density-sex ratios. We collected
¹⁴⁷ the number of panicles from a subset of females in each plot and collected the number of
¹⁴⁸ seeds in each panicle. Since the number of panicles (proxy of reproduction effort) does not nec-
¹⁴⁹ essarily reflect reproduction success in *Poar arachnifera*, we accessed reproduction success (seed
¹⁵⁰ fertilized) using greenhouse-based germination and trazolium-based seed viability assays.

¹⁵¹ We used the sex-ratio to estimate the probability of viability and the germination rate.
¹⁵² Seed viability was modeled with a binomial distribution where the probability of viability
¹⁵³ (v) was given by:

$$v = v_0 * (1 - OSR^\alpha) \quad (1)$$

¹⁵⁵ where OSR is the operational sex ratio (proportion of panicles that were female) in the
¹⁵⁶ experimental populations. The properties of the above function is supported by our previous
¹⁵⁷ work (Compagnoni et al., 2017). Here, seed viability is maximized at v_0 as OSR approaches
¹⁵⁸ zero (strongly male-biased) and goes to zero as OSR approaches 1 (strongly female-biased).
¹⁵⁹ Parameter α controls how viability declines with increasing female bias.

¹⁶⁰ We used a binomial distribution to model the germination data from greenhouse trials.
¹⁶¹ Given that germination was conditional on seed viability, the probability of success was given
¹⁶² by the product $v * g$, where v is a function of OSR (Eq. 1) and g is assumed to be constant.

¹⁶³ Sex specific demographic responses to climate

¹⁶⁴ We used individual level measurements of survival, growth (number of tillers), flowering, num-
¹⁶⁵ ber of panicles to independently develop Bayesian mixed effect models describing how each
¹⁶⁶ vital rate varies as a function of sex, size, precipitation of growing and dormant season and tem-
¹⁶⁷ perature of of growing and dormant season. We fit vital rate models with second-degree poly-
¹⁶⁸ nomial functions for the influence of climate. We included a second-degree polynomial because
¹⁶⁹ we expected that climate variables would affect vital rates through a hump-shaped relationship.

¹⁷⁰ We centered and standardized all predictors to facilitate model convergence. We included
¹⁷¹ site, source, and block as random effect. All the vital rate models used the same linear and
¹⁷² quadratic predictor for the expected value (μ) (Eq. 2). However, we applied a different
¹⁷³ link function ($f(\mu)$) depending on the distribution the vital rate. We modeled survival and
¹⁷⁴ flowering data with a Bernoulli distribution. We modeled the growth (tiller number) with
¹⁷⁵ a zero-truncated Poisson inverse Gaussian distribution. Fertility (panicle count) was model

176 as zero-truncated negative binomial.

$$\begin{aligned} f(\mu) = & \beta_0 + \beta_1 size + \beta_2 sex + \beta_3 pptgrow + \beta_4 pptdorm + \beta_5 tempgrow + \beta_6 tempdorm \\ & + \beta_7 pptgrow * sex + \beta_8 pptdorm * sex + \beta_9 tempgrow * sex + \beta_{10} tempdorm * sex \\ & + \beta_{11} size * sex + \beta_{12} pptgrow * tempgrow + \beta_{13} pptdorm * tempdorm \\ & + \beta_{14} pptgrow * tempdorm * sex + \beta_{15} pptdorm * tempdorm * sex + \beta_{16} pptgrow^2 \\ & + \beta_{17} pptdorm^2 + \beta_{18} tempgrow^2 + \beta_{19} tempdorm^2 + \beta_{20} pptgrow^2 * sex \\ & + \beta_{21} pptdorm^2 * sex + \beta_{22} tempgrow^2 * sex + \beta_{23} tempdorm^2 * sex + \phi + \rho + \nu \end{aligned} \quad (2)$$

177
178 where β_0 is the grand mean intercept, $\beta_1 \dots \beta_{13}$ represent the size and climate dependent slopes.
179 *size* was on a natural logarithm scale. *pptgrow* is the precipitation of the growing season
180 (standardized to mean zero and unit variance), *tempgrow* is the temperature of the growing
181 season (standardized to mean zero and unit variance), *pptdorm* is the precipitation of the
182 dormant season (standardized to mean zero and unit variance), *tempdorm* is the temperature
183 of the dormant season (standardized to mean zero and unit variance). The model also
184 includes normally distributed random effects for block-to-block variation ($\phi \sim N(0, \sigma_{block})$) and
185 source-to-source variation that is related to the provenence of the seeds used to establish the
186 common garden ($\rho \sim N(0, \sigma_{source})$), site to site variation ($\nu \sim N(0, \sigma_{site})$). We fit survival, growth,
187 flowering models with generic weakly informative priors for coefficients ($\mu = 0, \sigma = 1.5$) and
188 variances ($\gamma[0.1, 0.1]$). **We fit fertility model with different generic weakly informative priors**
189 **for coefficients ($\mu = 0, \sigma = 0.15$)**. We ran three chains for 1000 samples for warmup and 4000
190 for interactions, with a thinning rate of 3. We accessed the quality of the models using trace
191 plots and predictive check graphs (Piironen and Vehtari, 2017) (Supporting Information S-2).
192 To understand the effect of climate on vital rates, we got the 95 % credible interval of the
193 posterior distribution. Then we assumed that there is 95 % probability that the true (unknown)
194 estimates would lie within that interval, given the evidence provided by the observed data
195 for each vital rate. All models were fit in Stan (Stan Development Team, 2023).

196 Population growth rate responses to climate

197 To understand the effect of climate on population growth rate, we used the vital rate estimated
198 earlier to build a matrix projection model (MPM) structured by size (number of tillers), sex
199 and climate as covariate. Let $F_{x,z,t}$ and $M_{x,z,t}$ be the number of female and male plants of
200 size x in year t present at a location that has z as climate, where $x \in \{1, 2, \dots, U\}$ and U is the
201 maximum number of tillers a plant can reach (here 95th percentile of observed maximum
202 size). Let F_t^R and M_t^R be the new recruits, which we assume do not reproduce in their first

203 year. We assume that the parameters of sex ratio-dependent mating (Eq. 1) do not vary with
 204 climate. For a pre-breeding census, the expected numbers of recruits in year $t+1$ is given by:

$$205 \quad F_{t+1}^R = \sum_{x=1}^U [p^F(x,z) \cdot c^F(x,z) \cdot d \cdot v(\mathbf{F}_t, \mathbf{M}_t) \cdot m \cdot \rho] F_{x,z,t} \quad (3)$$

$$206 \quad M_{t+1}^R = \sum_{x=1}^U [p^F(x,z) \cdot c^F(x,z) \cdot d \cdot v(\mathbf{F}_t, \mathbf{M}_t) \cdot m \cdot (1-\rho)] F_{x,z,t} \quad (4)$$

207 where p^F and c^F are flowering probability and panicle production for females of size x , d
 208 is the number of seeds per female panicle, v is the probability that a seed is fertilized, m is
 209 the probability that a fertilized seed germinates, and ρ is the primary sex ratio (proportion
 210 of recruits that are female), z is the climate. Seed fertilization depends on the OSR of panicles
 211 (following Eq. 1) which was derived from the $U \times 1$ vectors of population structure \mathbf{F}_t and \mathbf{M}_t :

$$212 \quad v(\mathbf{F}_t, \mathbf{M}_t) = v_0 * \left[1 - \left(\frac{\sum_{x=1}^U p^F(x,z) c^F(x,z) F_{x,z,t}}{\sum_{x=1}^U p^F(x,z) c^F(x,z) F_{x,z,t} + p^M(x,z) c^M(x,z) M_{x,z,t}} \right)^\alpha \right] \quad (5)$$

213 Thus, the dynamics of the size-structured component of the population are given by:

$$214 \quad F_{y,t+1} = [\sigma \cdot g^F(y, x=1, z)] F_t^R + \sum_{x=1}^U [s^F(x,z) \cdot g^F(y, x, z)] F_{x,z,t} \quad (6)$$

$$215 \quad M_{y,t+1} = [\sigma \cdot g^M(y, x=1, z)] M_t^R + \sum_{x=1}^U [s^M(x,z) \cdot g^M(y, x, z)] M_{x,z,t} \quad (7)$$

216 In the two formula above, the first term represents seedlings that survived their first year
 217 and enter the size distribution of established plants. Instead of using *P. arachnifera* survival
 218 probability, we used the seedling survival probability (σ) from demographic studies of the
 219 hermaphroditic congener *Poa autumnalis* in east Texas (T.E.X. Miller and J.A. Rudgers, *unpub-*
 220 *lished data*), and we assume this probability was constant across sexes and climatic variables. We
 221 did this because we had little information on the early life cycle transitions of greenhouse-raised
 222 transplants. We also assume that $g(y, x=1)$ is the probability that a surviving seedlings reach
 223 size y , the expected future size of 1-tiller plants from the transplant experiment. The second
 224 term represents survival and size transition of established plants from the previous year, where
 225 s and g give the probabilities of surviving at size x and growing from sizes x to y , respectively,
 226 and superscripts indicate that these functions may be unique to females (F) and males (M).

227 Because the two-sex MPM is nonlinear (vital rates affect and are affected by population
 228 structure) we estimated the asymptotic geometric growth rate (λ) by numerical simulation,
 229 and repeated this across a range of climate.

230 **Identifying the mechanisms of population growth rate sensitivity to climate**

231 ⁴ To identify which aspect of climate is most important for population viability, we use
232 a "random design" Life Table Response Experiment (LTRE). We used the RandomForest
233 package to fit a regression model with θ as predictors and λ_c as response (Ellner et al., 2016;
234 Liaw et al., 2002). The LTRE approximates the variation in λ in response to climate covariates
235 and their interaction (Caswell, 2000; Hernández et al., 2023):

236

$$Var(\lambda_c) \approx \sum_{i=-1}^n \sum_{j=1}^n Cov(\theta_i, \theta_j, \theta_{ij}) + Var(\epsilon) \quad (8)$$

237 where, θ_i , θ_j , θ_{ij} represent respectively the fitted regression slope for the covariate of the
238 dormant season, j the covariate of the growing season and ij the covariate of their interactions.

239 Because LTRE contributions are additive, we summed across vital rates to compare the
240 total contributions of female and male parameters.

241 **Implication of climate change on range shifts**

242 To understand the implication of our study on range, we extrapolate population growth
243 using past, current and future climatic data across the range to map species distributions.
244 Averaging projection of population growth rates was used to reduce uncertainty across
245 climate projections (general circulation models).

246 All the analysis were performed in R 4.3.1 (R Core Team, 2023)

247 **Results**

248 **Sex specific demographic response to climate change**

249 Most vital rates were strongly climate dependent, but the magnitude of their response differed
250 between sexes suggesting a sex-specific demographic response to climate. Survival and
251 flowering were strongly more dependent on climate than growth (number of tillers) and repro-
252 duction (number of panicles) (Fig.1; Supporting Information S-3). We found opposite patterns
253 in the direction of the effect on seasonal climate on the probability of survival and flowering.
254 The growing season (precipitation) has a negative effect on the probability of survival, number
255 of tillers, and the probability of flowering, whereas the dormant season has a positive effect
256 on these vital rates. Unlike the other seasonal variables, temperature had different effects on

⁴I don't think the LTRE analysis is adequately motivated by the Intro.

257 different vital rates. Temperature of the growing season has a positive effect of the probability
258 of survival, a negative effect of the probability of flowering, and the number of tillers, but no
259 significant effect on the number of panicles. Further, there was a female survival and flowering
260 advantage across both climatic seasons (Figures. 3A-3D, 3I-3K). On the contrary, there was
261 a male panicle advantage across all climatic variables (Figure3M-3P). Counter-intuitively, there
262 was no significant sex growth advantage in all season climatic variables (Figures. 3E-3H).

263 **Population growth rate response to climate change**

264 We estimated the predicted response to population growth rate (population fitness) to seasonal
265 climate gradients using a model assuming a female dominant model and another model using
266 the two sexes. Consistent with the effect of climate on the individual vital rate, we found a
267 strong effect of seasonal climate on population fitness (Fig.2). For both models (female domi-
268 nant and two sexes), population fitness decreased with an increase of precipitation of growing
269 season. In contrast population fitness increased with precipitation of the dormant season. Fur-
270 thermore, population fitness was maximized between 23 and 17 degrees Celsius and decreases
271 to zero just beyond 32 degrees Celsius during the growing season. Similarly population fitness
272 was maximized between 13 and 17 degrees Celsius and decreases to zero just beyond 20 de-
273 grees Celsius during the growing season. We have also detected a strong effect of the past and
274 future climate on population growth rate. However, for future climate, the magnitude of that ef-
275 fect was different between gas-scenario emissions. A moderate emission gas scenario (RCP4.5)
276 has a moderate effect on the population growth rate, while a high emission scenario (RCP8.5)
277 has a strong effect on the population growth rate. High-emission scenario (RCP8.5) will lead
278 to an alteration of population viability. Under past climate conditions, population growth rate
279 decreased below one for temperature of the growing season and the dormant season.

280 **Climatic niches and range predictions**

281 Our demographically based range predictions broadly captured the known distribution of
282 the species (Fig. 1). More specifically, the predicted population viable ($\lambda > 1$) matches the
283 presence and absence of the species. Furthermore, viable populations of *P. arichnifera* were
284 only predicted at the center of the range for current climatic conditions (Fig1). Future and
285 past projections of climate change showed a north-west range shift compared to current
286 distributions. Although *P. arichnifera* was predicted to have suitable habitat in the center of the
287 range under the current climate, future warming is predicted to reduce much of the suitable
288 habitat in the southern part (Figure).

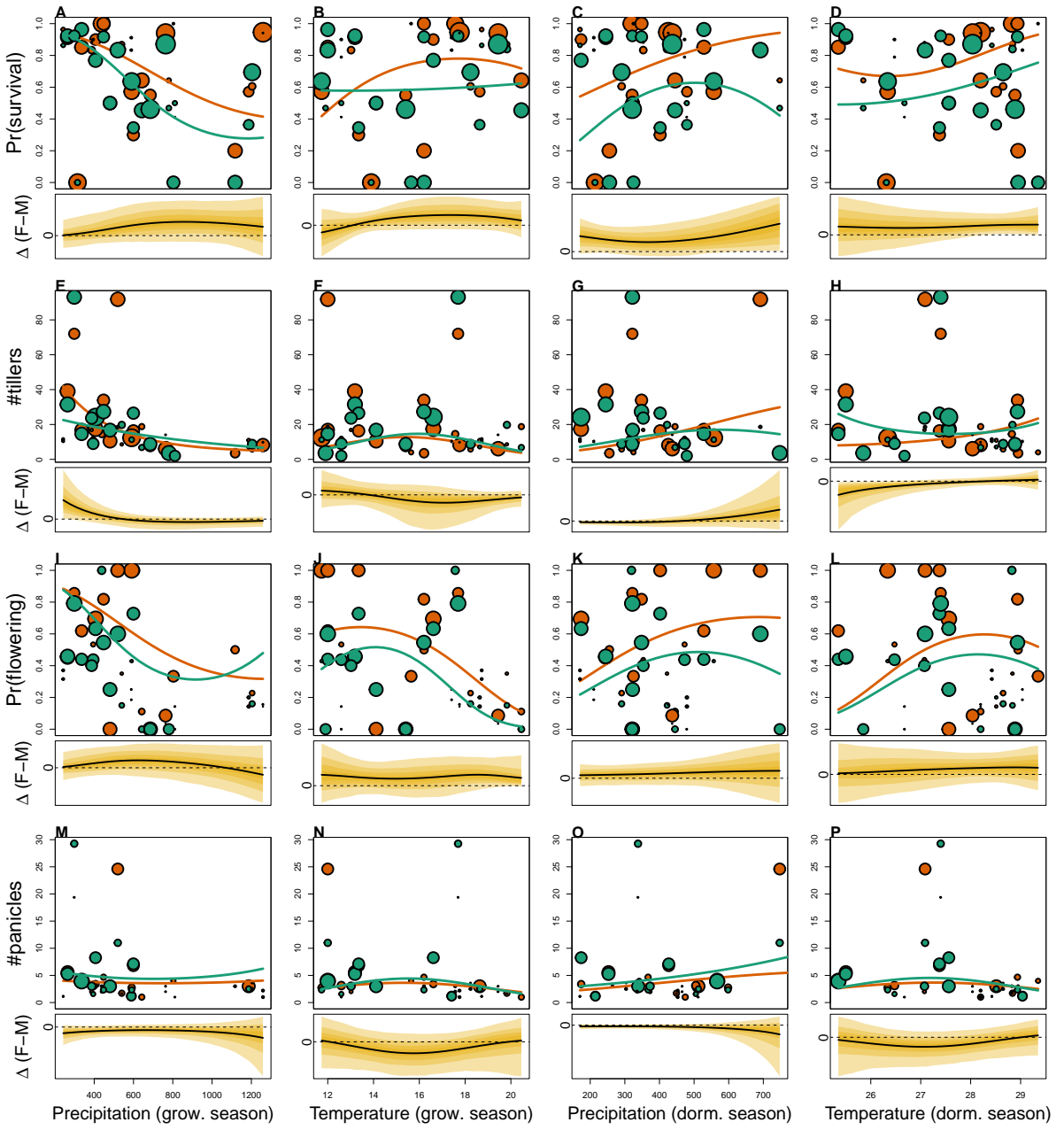


Figure 1: Sex specific demographic response to climate across species range: A–D, inter-annual probability of survival; E–H, inter-annual growth (change in number of tillers); I–L, probability of flowering; M–P, number of panicles produced given flowering. Points show means by site for females (orange) and males (green). Point size is proportional to the sample size of the mean. Lines show fitted statistical models for females (yellow) and males (green) based on posterior mean parameter values. Lower panels below each data panel show the posterior distribution of the difference between females and males as a function of climate (positive and negative values indicate female and male advantage, respectively); dashed horizontal line shows zero difference.

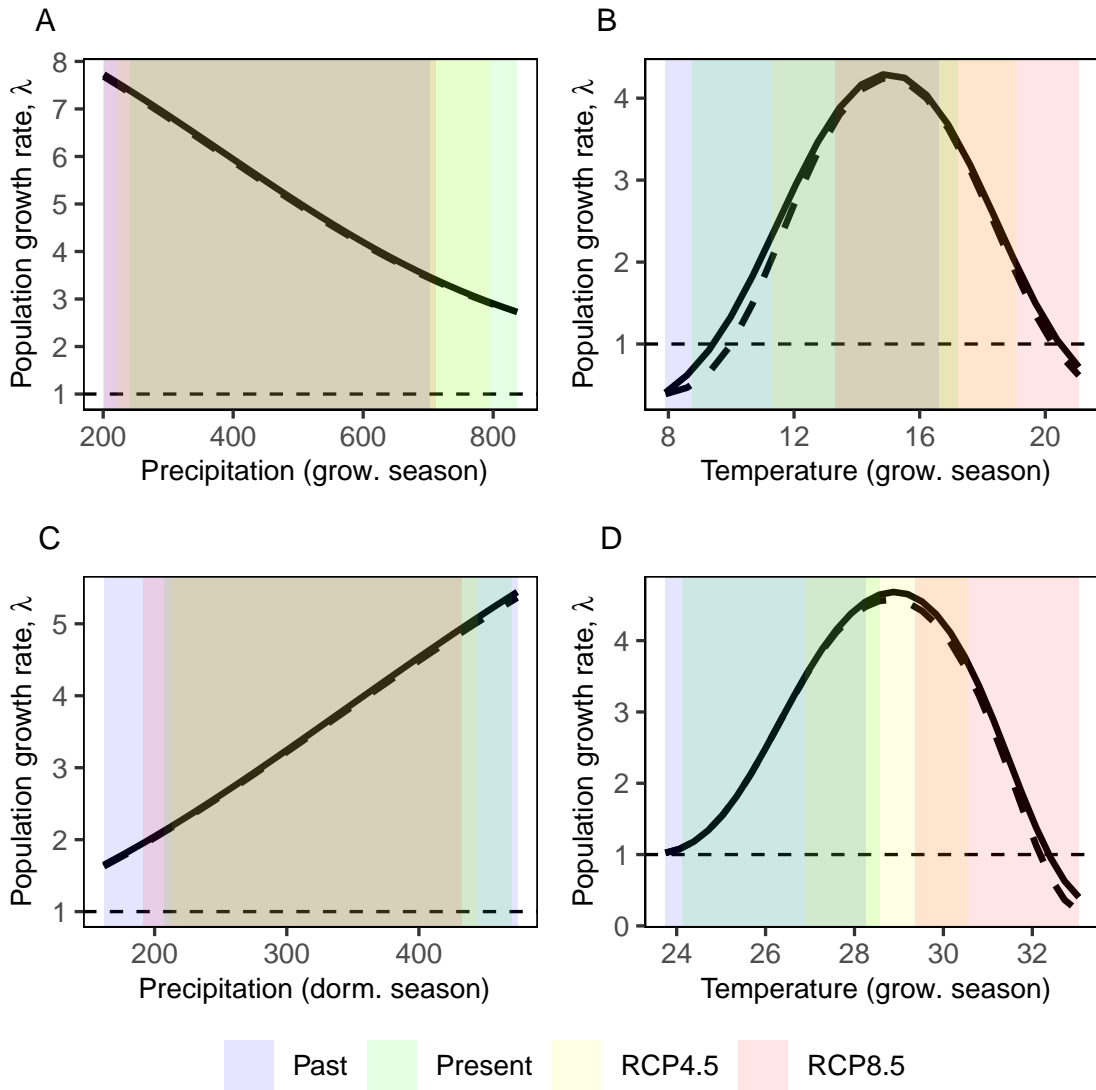


Figure 2: Population growth rate (λ) as a function of climate (past climate, present and predicted future climates). For future climate, we show a Representation Concentration Pathways 4.5 and 8.5. Values of (λ) are derived from the mean climate variables across 4 GCMs. The solid bold curve shows prediction by the two-sex matrix projection model that incorporates sex- specific demographic responses to climate with sex ratio dependent seed fertilization. The bold dashed curve represents the prediction by the female dominant matrix projection model. The dashed horizontal line indicates the limit of population viability ($\lambda = 1$)

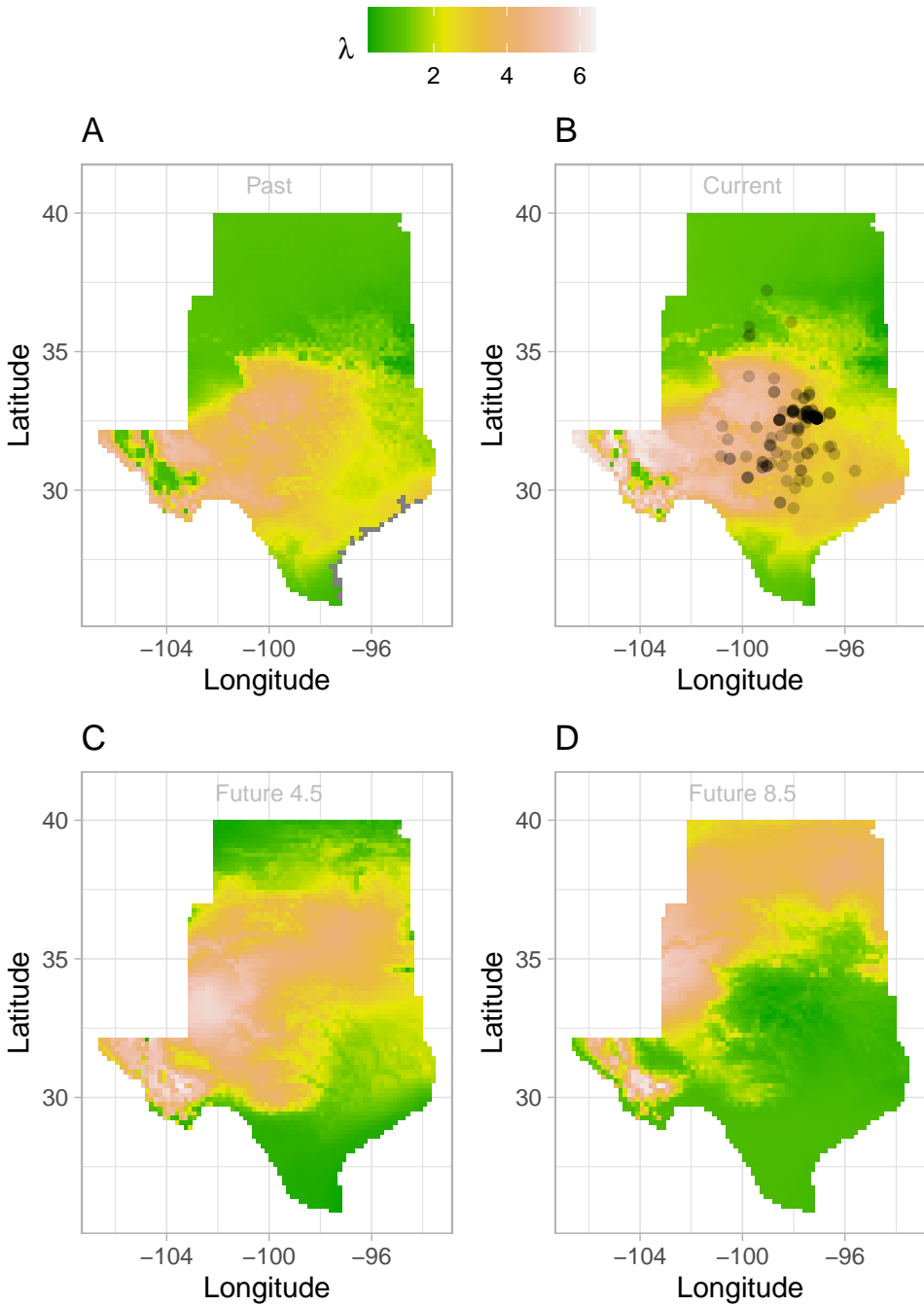


Figure 3: Past (A), Current (B), Future (2070–20100) (C and D) predicted range shift based on population growth rate. Future projections were based on the average population growth rate in four GCMs. The black circles on panel B indicate all known presence points collected from GBIF from 1990 to 2019, which corresponds to the current condition in our prediction. The occurrences of GBIFs are distributed inwith higher population fitness habitat ($\lambda > 1$) , confirming that our study approach can reasonably predict range shifts.

289 **Discussion**

290 **References**

- 291 Bertrand, R., Lenoir, J., Piedallu, C., Riofrío-Dillon, G., De Ruffray, P., Vidal, C., Pierrat, J.-C.,
292 and Gégout, J.-C. (2011). Changes in plant community composition lag behind climate
293 warming in lowland forests. *Nature*, 479(7374):517–520.
- 294 Bürli, S., Pannell, J. R., and Tonnabel, J. (2022). Environmental variation in sex ratios and
295 sexual dimorphism in three wind-pollinated dioecious plant species. *Oikos*, 2022(6):e08651.
- 296 Caswell, H. (2000). *Matrix population models*, volume 1. Sinauer Sunderland, MA.
- 297 Compagnoni, A., Steigman, K., and Miller, T. E. (2017). Can't live with them, can't live
298 without them? balancing mating and competition in two-sex populations. *Proceedings of
299 the Royal Society B: Biological Sciences*, 284(1865):20171999.
- 300 Czachura, K. and Miller, T. E. (2020). Demographic back-casting reveals that subtle
301 dimensions of climate change have strong effects on population viability. *Journal of Ecology*,
302 108(6):2557–2570.
- 303 Dahlgren, J. P., Bengtsson, K., and Ehrlén, J. (2016). The demography of climate-driven and
304 density-regulated population dynamics in a perennial plant. *Ecology*, 97(4):899–907.
- 305 Davis, M. B. and Shaw, R. G. (2001). Range shifts and adaptive responses to quaternary
306 climate change. *Science*, 292(5517):673–679.
- 307 Eberhart-Phillips, L. J., Küpper, C., Miller, T. E., Cruz-López, M., Maher, K. H., Dos Remedios,
308 N., Stoffel, M. A., Hoffman, J. I., Krüger, O., and Székely, T. (2017). Sex-specific early
309 survival drives adult sex ratio bias in snowy plovers and impacts mating system and
310 population growth. *Proceedings of the National Academy of Sciences*, 114(27):E5474–E5481.
- 311 Ellis, R. P., Davison, W., Queirós, A. M., Kroeker, K. J., Calosi, P., Dupont, S., Spicer, J. I.,
312 Wilson, R. W., Widdicombe, S., and Urbina, M. A. (2017). Does sex really matter? explaining
313 intraspecies variation in ocean acidification responses. *Biology letters*, 13(2):20160761.
- 314 Ellner, S. P., Childs, D. Z., Rees, M., et al. (2016). Data-driven modelling of structured
315 populations. *A practical guide to the Integral Projection Model*. Cham: Springer.
- 316 Evans, M. E., Merow, C., Record, S., McMahon, S. M., and Enquist, B. J. (2016). Towards
317 process-based range modeling of many species. *Trends in Ecology & Evolution*, 31(11):860–871.

- 318 Gamelon, M., Grøtan, V., Nilsson, A. L., Engen, S., Hurrell, J. W., Jerstad, K., Phillips, A. S.,
319 Røstad, O. W., Slagsvold, T., Walseng, B., et al. (2017). Interactions between demography
320 and environmental effects are important determinants of population dynamics. *Science*
321 *Advances*, 3(2):e1602298.
- 322 Gissi, E., Schiebinger, L., Hadly, E. A., Crowder, L. B., Santoleri, R., and Micheli, F. (2023a).
323 Exploring climate-induced sex-based differences in aquatic and terrestrial ecosystems to
324 mitigate biodiversity loss. *nature communications*, 14(1):4787.
- 325 Gissi, E., Schiebinger, L., Santoleri, R., and Micheli, F. (2023b). Sex analysis in marine biological
326 systems: insights and opportunities. *Frontiers in Ecology and the Environment*.
- 327 Hernández, C. M., Ellner, S. P., Adler, P. B., Hooker, G., and Snyder, R. E. (2023). An exact
328 version of life table response experiment analysis, and the r package exactltre. *Methods*
329 in *Ecology and Evolution*, 14(3):939–951.
- 330 Hitchcock, A. S. (1971). *Manual of the grasses of the United States*, volume 2. Courier Corporation.
- 331 Hultine, K. R., Grady, K. C., Wood, T. E., Shuster, S. M., Stella, J. C., and Whitham, T. G. (2016).
332 Climate change perils for dioecious plant species. *Nature Plants*, 2(8):1–8.
- 333 Jones, M. H., Macdonald, S. E., and Henry, G. H. (1999). Sex-and habitat-specific responses
334 of a high arctic willow, *salix arctica*, to experimental climate change. *Oikos*, pages 129–138.
- 335 Karger, D. N., Conrad, O., Böhner, J., Kawohl, T., Kreft, H., Soria-Auza, R. W., Zimmermann,
336 N. E., Linder, H. P., and Kessler, M. (2017). Climatologies at high resolution for the earth's
337 land surface areas. *Scientific data*, 4(1):1–20.
- 338 Kindiger, B. (2004). Interspecific hybrids of *poa arachnifera* × *poa secunda*. *Journal of New*
339 *Seeds*, 6(1):1–26.
- 340 Lee-Yaw, J. A., Kharouba, H. M., Bontrager, M., Mahony, C., Csergő, A. M., Noreen, A. M.,
341 Li, Q., Schuster, R., and Angert, A. L. (2016). A synthesis of transplant experiments and
342 ecological niche models suggests that range limits are often niche limits. *Ecology letters*,
343 19(6):710–722.
- 344 Leicht-Young, S. A., Silander, J. A., and Latimer, A. M. (2007). Comparative performance of
345 invasive and native *celastrus* species across environmental gradients. *Oecologia*, 154:273–282.
- 346 Liaw, A., Wiener, M., et al. (2002). Classification and regression by randomforest. *R news*,
347 2(3):18–22.

- 348 Louthan, A. M., Keighron, M., Kiekebusch, E., Cayton, H., Terando, A., and Morris, W. F.
349 (2022). Climate change weakens the impact of disturbance interval on the growth rate of
350 natural populations of venus flytrap. *Ecological Monographs*, 92(4):e1528.
- 351 Merow, C., Bois, S. T., Allen, J. M., Xie, Y., and Silander Jr, J. A. (2017). Climate change both
352 facilitates and inhibits invasive plant ranges in new england. *Proceedings of the National
353 Academy of Sciences*, 114(16):E3276–E3284.
- 354 Miller, T. and Compagnoni, A. (2022a). Data from: Two-sex demography, sexual niche
355 differentiation, and the geographic range limits of texas bluegrass (*Poa arachnifera*). *American
356 Naturalist, Dryad Digital Repository*,. <https://doi.org/10.5061/dryad.kkwh70s5x>.
- 357 Miller, T. E. and Compagnoni, A. (2022b). Two-sex demography, sexual niche differentiation,
358 and the geographic range limits of texas bluegrass (*poa arachnifera*). *The American
359 Naturalist*, 200(1):17–31.
- 360 Morrison, C. A., Robinson, R. A., Clark, J. A., and Gill, J. A. (2016). Causes and consequences
361 of spatial variation in sex ratios in a declining bird species. *Journal of Animal Ecology*,
362 85(5):1298–1306.
- 363 Pease, C. M., Lande, R., and Bull, J. (1989). A model of population growth, dispersal and
364 evolution in a changing environment. *Ecology*, 70(6):1657–1664.
- 365 Petry, W. K., Soule, J. D., Iler, A. M., Chicas-Mosier, A., Inouye, D. W., Miller, T. E., and
366 Mooney, K. A. (2016). Sex-specific responses to climate change in plants alter population
367 sex ratio and performance. *Science*, 353(6294):69–71.
- 368 Piironen, J. and Vehtari, A. (2017). Comparison of bayesian predictive methods for model
369 selection. *Statistics and Computing*, 27:711–735.
- 370 Pottier, P., Burke, S., Drobniak, S. M., Lagisz, M., and Nakagawa, S. (2021). Sexual (in) equality?
371 a meta-analysis of sex differences in thermal acclimation capacity across ectotherms.
372 *Functional Ecology*, 35(12):2663–2678.
- 373 R Core Team (2023). *R: A Language and Environment for Statistical Computing*. R Foundation
374 for Statistical Computing, Vienna, Austria.
- 375 Sanderson, B. M., Knutti, R., and Caldwell, P. (2015). A representative democracy to reduce
376 interdependency in a multimodel ensemble. *Journal of Climate*, 28(13):5171–5194.

- 377 Sasaki, M., Hedberg, S., Richardson, K., and Dam, H. G. (2019). Complex interactions
378 between local adaptation, phenotypic plasticity and sex affect vulnerability to warming
379 in a widespread marine copepod. *Royal Society open science*, 6(3):182115.
- 380 Schwalm, C. R., Glendon, S., and Duffy, P. B. (2020). Rcp8. 5 tracks cumulative co2 emissions.
381 *Proceedings of the National Academy of Sciences*, 117(33):19656–19657.
- 382 Schwinning, S., Lortie, C. J., Esque, T. C., and DeFalco, L. A. (2022). What common-garden
383 experiments tell us about climate responses in plants.
- 384 Sexton, J. P., McIntyre, P. J., Angert, A. L., and Rice, K. J. (2009). Evolution and ecology of
385 species range limits. *Annu. Rev. Ecol. Evol. Syst.*, 40:415–436.
- 386 Smith, M. D., Wilkins, K. D., Holdrege, M. C., Wilfahrt, P., Collins, S. L., Knapp, A. K., Sala,
387 O. E., Dukes, J. S., Phillips, R. P., Yahdjian, L., et al. (2024). Extreme drought impacts have
388 been underestimated in grasslands and shrublands globally. *Proceedings of the National
389 Academy of Sciences*, 121(4):e2309881120.
- 390 Stan Development Team (2023). RStan: the R interface to Stan. R package version 2.21.8.
- 391 Thomson, A. M., Calvin, K. V., Smith, S. J., Kyle, G. P., Volke, A., Patel, P., Delgado-Arias,
392 S., Bond-Lamberty, B., Wise, M. A., Clarke, L. E., et al. (2011). Rcp4. 5: a pathway for
393 stabilization of radiative forcing by 2100. *Climatic change*, 109:77–94.
- 394 Tognetti, R. (2012). Adaptation to climate change of dioecious plants: does gender balance
395 matter? *Tree Physiology*, 32(11):1321–1324.
- 396 Welbergen, J. A., Klose, S. M., Markus, N., and Eby, P. (2008). Climate change and the
397 effects of temperature extremes on australian flying-foxes. *Proceedings of the Royal Society
398 B: Biological Sciences*, 275(1633):419–425.
- 399 Zhao, H., Li, Y., Zhang, X., Korpelainen, H., and Li, C. (2012). Sex-related and stage-dependent
400 source-to-sink transition in populus cathayana grown at elevated co 2 and elevated
401 temperature. *Tree Physiology*, 32(11):1325–1338.

Supporting Information

402 S.1 XX

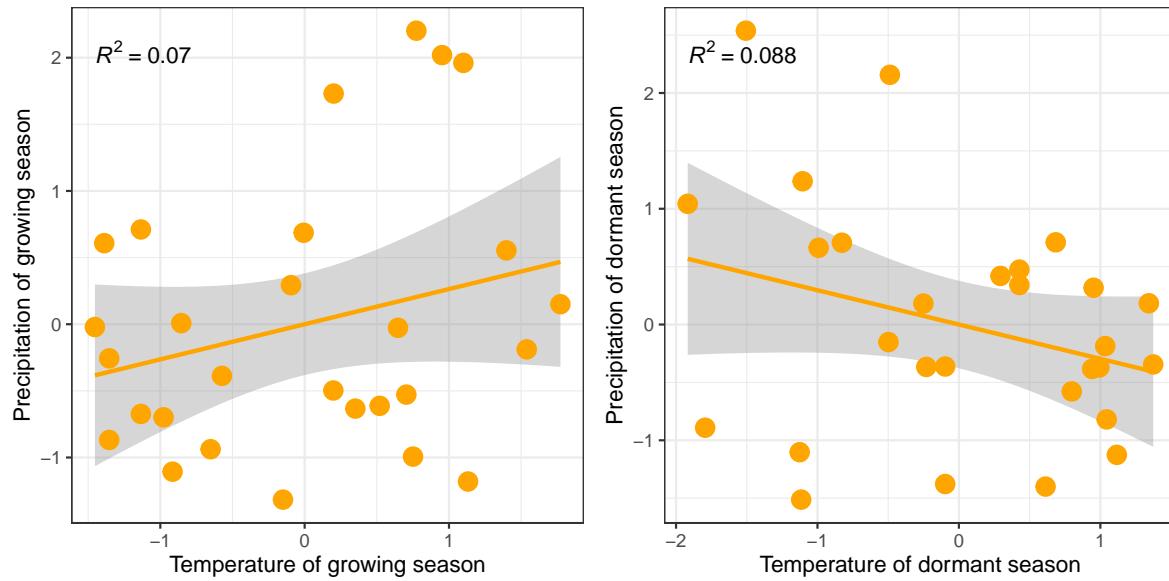


Figure S-1: Relation between precipitation and temperature for each season (growing and dormant). R^2 indicates the value of proportion of explained variance between the temperature and precipitation

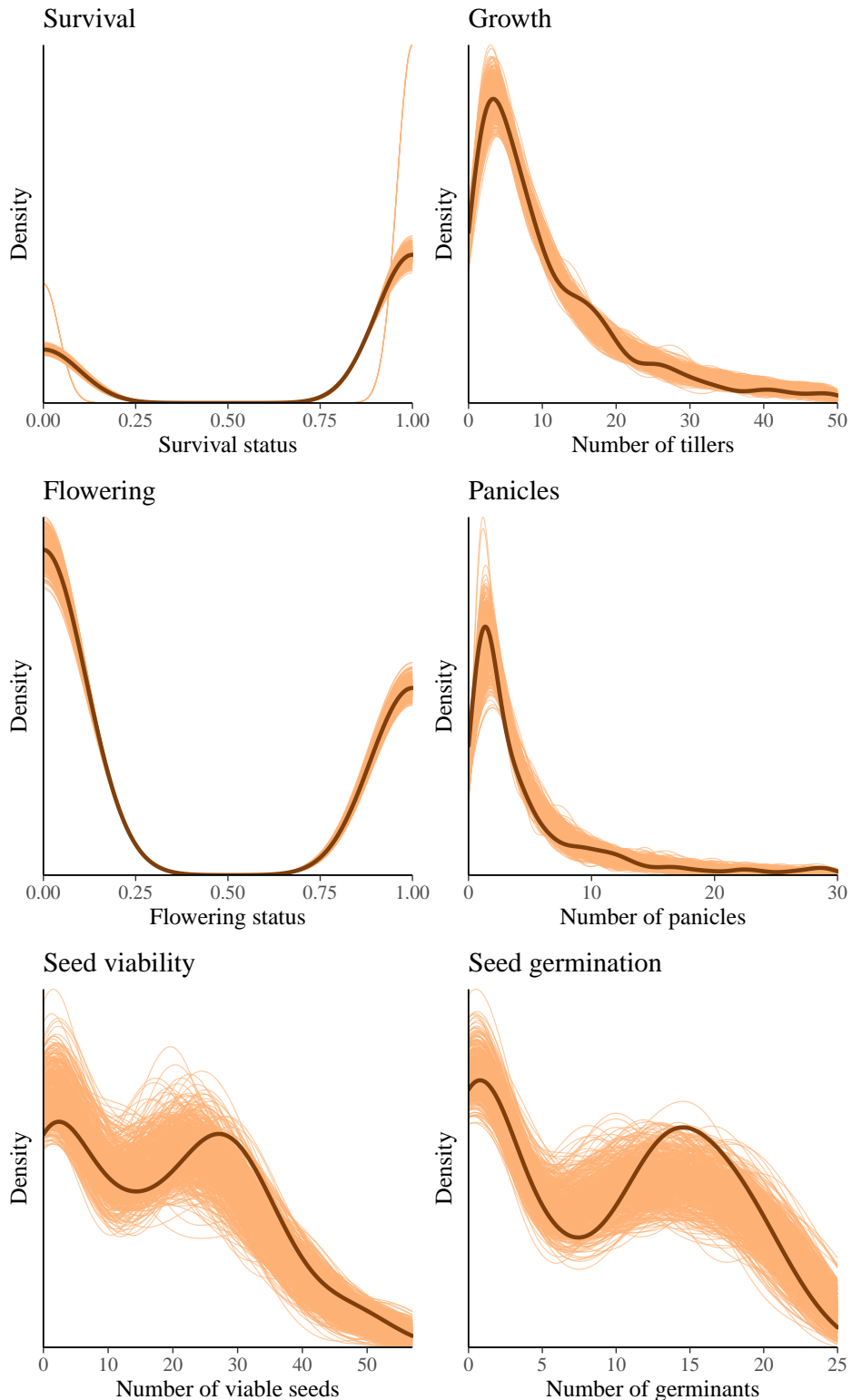


Figure S-2: Consistency between real data and simulated values suggests that the fitted model accurately describes the data. Graph shows density curves for the observed data (light blue) along with the simulated values (dark blue). The first column shows the linear models and the second column shows the 2 degree polynomial models.

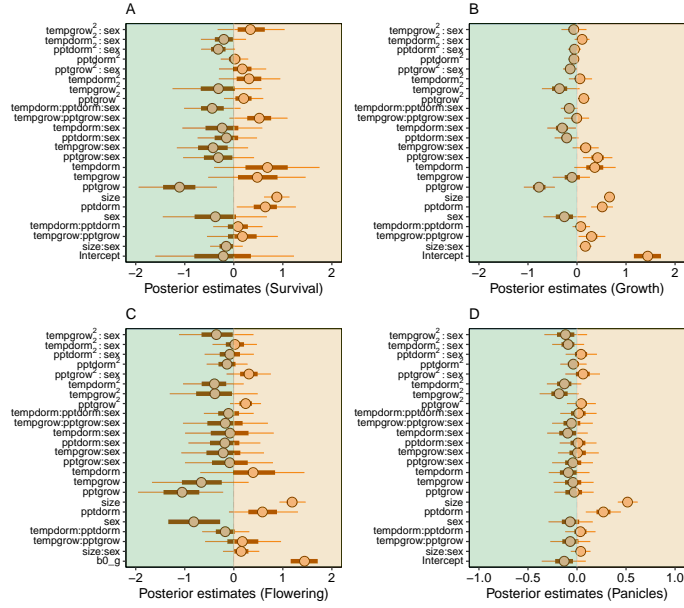


Figure S-3: Mean parameter values and 95% credible intervals for all vital rates.

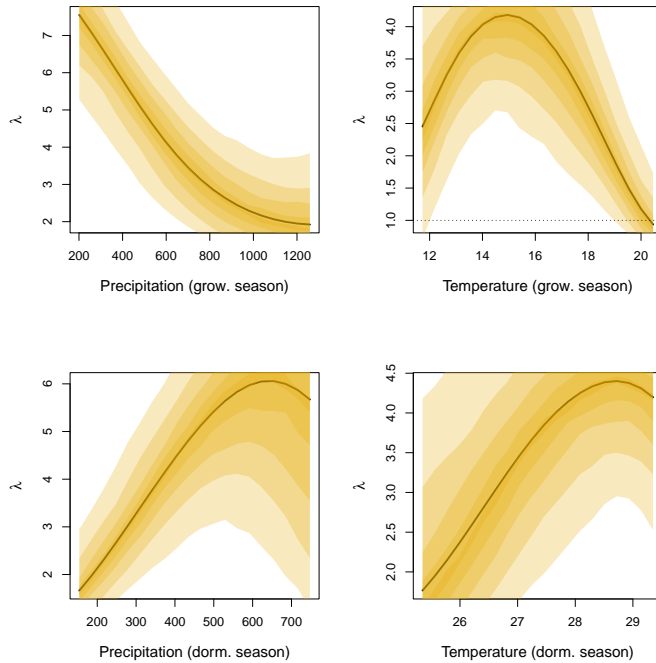


Figure S-4: Population growth rate (λ) as a function of seasonal climate (2016-2017), predicted by the two-sex matrix projection model that incorporates sex-specific demographic responses to climate with sex ratio-dependent seed fertilization. We show the mean posterior distribution of λ in solid lines, and the 5, 25, 50, 75, and 95% percentiles of parameter uncertainty in shaded gold color. The dashed horizontal line indicates the limit of population viability ($\lambda = 1$)

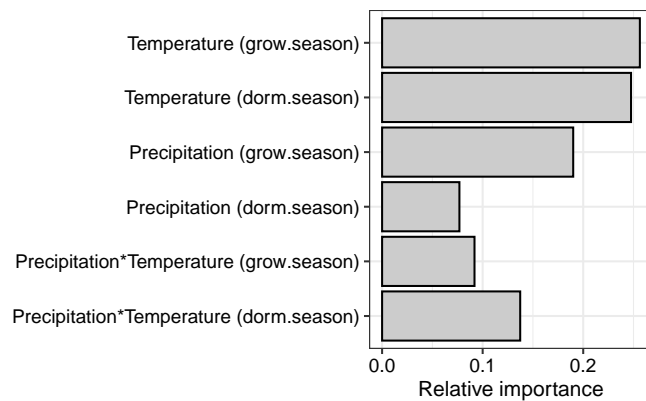


Figure S-5: XXX